

See discussions, stats, and author profiles for this publication at: <https://www.researchgate.net/publication/284477231>

Pyrolytic Carbon for Long-Term Medical Implants

Article · December 2013

DOI: 10.1016/B978-0-08-087780-8.00023-1

CITATIONS

9

READS

118

3 authors:



Robert More

22 PUBLICATIONS 336 CITATIONS

SEE PROFILE



Axel Haubold

Bed Rock Ranch

67 PUBLICATIONS 613 CITATIONS

SEE PROFILE



Jack Bokros

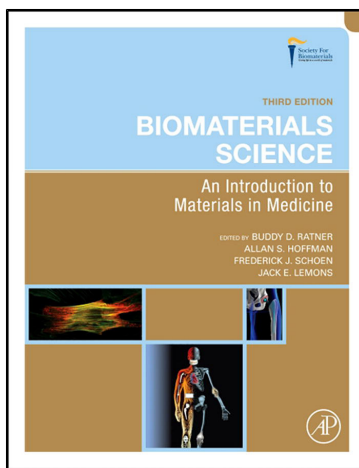
Life Technologies

89 PUBLICATIONS 1,114 CITATIONS

SEE PROFILE

**Provided for non-commercial research and educational use only.
Not for reproduction, distribution or commercial use.**

This chapter was originally published in the book *Biomaterials Science*. The copy attached is provided by Elsevier for the author's benefit and for the benefit of the author's institution, for non-commercial research, and educational use. This includes without limitation use in instruction at your institution, distribution to specific colleagues, and providing a copy to your institution's administrator.



All other uses, reproduction and distribution, including without limitation commercial reprints, selling or licensing copies or access, or posting on open internet sites, your personal or institution's website or repository, are prohibited. For exceptions, permission may be sought for such use through Elsevier's permissions site at:

<http://www.elsevier.com/locate/permissionusematerial>

From More R. B., Haubold A. D., & Bokros J. C. (2013). Pyrolytic carbon for long-term medical implants. In B. D. Ratner, A. S. Hoffman & F. J. Schoen (Eds.), *Biomaterials Science* (pp. 209–222). Elsevier Inc., Academic Press.
ISBN: 9780123746269

Copyright © 2013 Elsevier Inc. All rights reserved.
Academic Press

- Shu, X. Z., Liu, Y., Luo, Y., Roberts, M. C., & Prestwich, G. D. (2002). Disulfide cross-linked hyaluronan hydrogels. *Biomacromolecules*, 3(6), 1304–1311.
- Shin, H., Jo, S., & Mikos, A. G. (2003). Biomimetic materials for tissue engineering. *Biomaterials*, 24(24), 4353–4364.
- Shu, X. Z., Ghosh, K., Liu, Y., Palumbo, F. S., Luo, Y., et al. (2004). Attachment and spreading of fibroblasts on an RGD peptide-modified injectable hyaluronan hydrogel. *J. Biomed. Mater. Res. A*, 68(2), 365–375.
- Shu, X. Z., & Prestwich, G. D. (2004). Therapeutic Biomaterials from Chemically Modified Hyaluronan. In H. G. Garg, & C. A. Hales (Eds.), *Chemistry and Biology of Hyaluronan* (pp. 475–504). Amsterdam: Elsevier.
- Shu, X. Z., Ahmad, S., Liu, Y., & Prestwich, G. D. (2006). Synthesis and evaluation of injectable, *in situ* cross-linkable synthetic extracellular matrices for tissue engineering. *J. Biomed. Mater. Res. A*, 79(4), 902–912.
- Sondrup, C., Liu, Y., Shu, X. Z., Prestwich, G. D., & Smith, M. E. (2006). Cross-linked hyaluronan-coated stents in the prevention of airway stenosis. *Otolaryngol Head Neck Surg.*, 135(1), 28–35.
- Stenzel, K. H., Miyata, T., & Rubin, A. L. (1974). Collagen as a biomaterial. *Annu. Rev. Biophys. Bioeng.*, 3(0), 231–253.
- Stone, K. R., Steadman, J. R., Rodkey, W. G., & Li, S. T. (1997). Regeneration of meniscal cartilage with use of a collagen scaffold. Analysis of preliminary data. *J. Bone. Joint Surg. Am.*, 79(12), 1770–1777.
- Suh, J. K., & Matthew, H. W. (2000). Application of chitosan-based polysaccharide biomaterials in cartilage tissue engineering: A review. *Biomaterials*, 21(24), 2589–2598.
- Urry, D. W., Hugel, T., Seitz, M., Gaub, H. E., Sheiba, L., et al. (2002). Elastin: A representative ideal protein elastomer. *Philos. Trans. R. Soc. Lond. B Biol. Sci.*, 357(1418), 169–184.
- van der Giessen, W. J., van Beusekom, H. M., Eijgelshoven, M. H., Morel, M. A., & Serruys, P. W. (1998). Heparin-coating of coronary stents. *Semin. Interv. Cardiol.*, 3(3–4), 173–176.
- Vanderhooft, J. L., Mann, B. K., & Prestwich, G. D. (2007). Synthesis and characterization of novel thiol-reactive poly(ethylene glycol) cross-linkers for biomaterials. *Biomacromolecules*, 8, 2883–2889.
- VandeVord, P. J., Matthew, H. W., DeSilva, S. P., Mayton, L., Wu, B., et al. (2002). Evaluation of the biocompatibility of a chitosan scaffold in mice. *J. Biomed. Mater. Res.*, 59(3), 585–590.
- White, M. J., Kohno, I., Rubin, A. L., Stenzel, K. H., & Miyata, T. (1973). Collagen films: Effect of cross-linking on physical and biological properties. *Biomater. Med. Devices Artif. Organs*, 1(4), 703–715.
- Yuan, N., Tsai, R., Ho, M., Wang, D., Lai, J., et al. (2008). Fabrication and characterization of chondroitin sulfate-modified chitosan membranes for biomedical applications. *Desalination*, 23(1–3), 166–174.

CHAPTER I.2.8 PYROLYTIC CARBON FOR LONG-TERM MEDICAL IMPLANTS

Robert B. More,¹ Axel D. Haubold,² and Jack C. Bokros³

¹Integra Life Sciences, Austin, TX, USA

²Bed Rock Ranch, Decatur, TX, USA

³On-X Life Technologies, Inc, Austin, TX, USA

INTRODUCTION

Carbon materials are ubiquitous and of great interest because the majority of substances that make up living organisms are carbon compounds. Although many engineering materials and biomaterials are based on carbon or contain carbon in some form, elemental carbon itself is also an important and very successful biomaterial. Furthermore, there exists enough diversity in their structure and properties for elemental carbons to be considered as a unique class of materials beyond the traditional molecular carbon focus of organic chemistry, polymer chemistry, and biochemistry. Through a serendipitous interaction between researchers during the late 1960s the outstanding blood compatibility of a special form of elemental pyrolytic carbon deposited at high temperature in a fluidized bed was discovered. The material was found to have not only remarkable blood compatibility, but also the structural properties needed for long-term use in artificial heart valves (LaGrange et al., 1969). The blood compatibility of pyrolytic carbon was recognized empirically using the Gott vena cava ring test. This test involved implanting a small tube made of a candidate material in a canine vena cava and observing

the development of thrombosis within the tube in time. Prior to pyrolytic carbon, only surfaces coated with graphite, benzylalkonium chloride, and heparin would resist thrombus formation when exposed to blood for long periods. The incorporation of pyrolytic carbon in mechanical heart valve implants was declared “an exceptional event” (Sadeghi, 1987) because it added the durability and stability needed for heart valve prostheses to endure for a patient’s lifetime. The objective of this chapter is to present the elemental pyrolytic carbon materials currently used in the fabrication of medical devices, and to describe their manufacture, characterization, and properties.

ELEMENTAL CARBON

Elemental carbon is found in nature as two crystalline allotrophic forms: graphite and diamond. Elemental carbon also occurs as a spectrum of imperfect, turbostratic crystalline forms that range in degree of crystallinity from amorphous to the perfectly crystalline allotropes. Recently a third crystalline form of elemental carbon, the fullerene structure, has been discovered. The crystalline polymorphs of elemental carbon are shown in Figure I.2.8.1.

The properties of the elemental carbon crystalline forms vary widely according to their structure. Diamond with its tetrahedral sp³ covalent bonding is one of the hardest materials known. In the diamond crystal structure, covalent bonds of length 1.54 Å connect each carbon atom with its four nearest neighbors. This tetrahedral symmetry repeats in three dimensions throughout

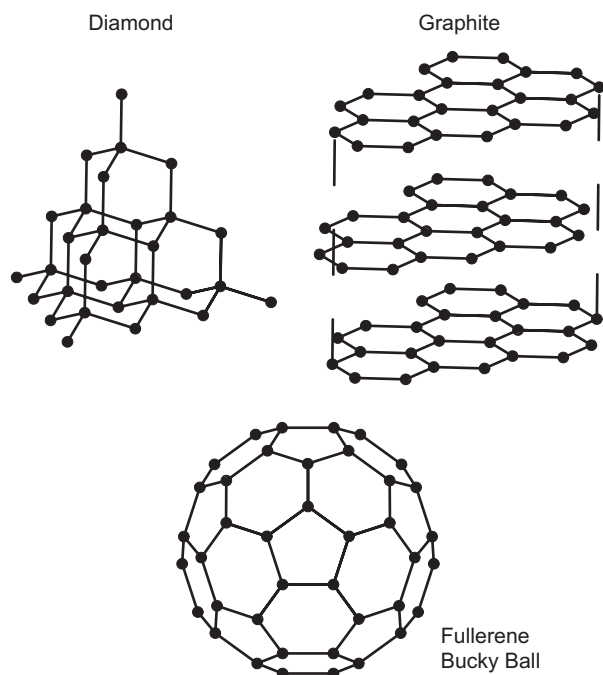


FIGURE 1.2.8.1 Allotropic crystalline forms of carbon: diamond, graphite, and fullerene.

the crystal (Pauling, 1964). In effect, the crystal is a giant isotropic covalently-bonded molecule; therefore, diamond is very hard.

Graphite, with its anisotropic layered in-plane hexagonal covalent bonding and interplane van der Waals bonding structure, is a soft material. Within each planar layer, each carbon atom forms two single bonds and one double bond with its three nearest neighbors. This bonding repeats in-plane to form a giant molecular (graphene) sheet. The in-plane atomic bond length is 1.42 Å, which is a resonant intermediate (Pauling, 1964) between the single bond length of 1.54 Å and the double bond length of 1.33 Å. The planer layers are held together by relatively weak van der Waals bonding at a distance of 3.4 Å, which is more than twice the 1.42 Å bond length (Pauling, 1964). Graphite has low hardness and a lubricating property because the giant molecular sheets can readily slip past one another against the van der Waals bonding. Nevertheless, although large-crystallite-size natural graphite is used as a lubricant, some artificially produced graphites can be very abrasive if the crystallite sizes are small and randomly oriented.

Fullerenes have yet to be produced in bulk, but their properties on a microscale are entirely different from those of their crystalline counterparts. Fullerenes and nanotubes consist of a graphene layer that is rolled up or folded (Sattler, 1995) to form a tube or ball. These large molecules, C_{60} and C_{70} fullerenes and $(C_{60} + 18j)$ nanotubes, are often mentioned in the literature (Sattler, 1995) along with more complex multilayer “onion skin” structures.

There exist many possible forms of elemental carbon that are intermediate in structure and properties

between those of the allotropes diamond and graphite. Such “turbostratic” carbons occur as a spectrum of amorphous, through mixed amorphous, graphite-like and diamond-like, to the perfectly crystalline allotropes (Bokros, 1969). Because of the dependence of properties upon structure, there can be considerable variability in properties for the turbostratic carbons. Glassy carbons and pyrolytic carbons, for example, are two turbostratic carbons with considerable differences in structure and properties. Consequently, it is not surprising that carbon materials are often misunderstood through oversimplification. Properties found in one type of carbon structure can be totally different in another type of structure. Therefore, it is very important to specify the exact nature and structure when discussing carbon.

PYROLYTIC CARBON (PyC)

The biomaterial known as pyrolytic carbon is not found in nature; it is manmade. The successful pyrolytic carbon biomaterial was developed at General Atomic during the late 1960s using a fluidized-bed reactor (Bokros, 1969). In the original terminology, this material was considered a low-temperature isotropic carbon (LTI carbon). Since the initial clinical implant of a pyrolytic carbon component in the DeBakey–Surgitool mechanical valve in 1968, 95% of the mechanical heart valves implanted worldwide have at least one structural component made of pyrolytic carbon. On an annual basis this translates into approximately 500,000 components (Haubold, 1994). Pyrolytic carbon components have been used in more than 25 different prosthetic heart valve designs since the late 1960s, and have accumulated a clinical experience in the order of 16 million patient-years. Clearly, pyrolytic carbon is one of the most successful, critical biomaterials both in function and application. Among the materials available for mechanical heart valve prostheses, pyrolytic carbon has the best combination of blood compatibility, physical and mechanical properties, and durability. However, the blood compatibility of pyrolytic carbon in heart valve applications is not perfect; chronic anticoagulant therapy is needed for patients with mechanical heart valves. Whether the need for anticoagulant therapy arises from the biocompatible properties of the material itself or from the particular hydrodynamic interaction of a given device and the blood remains to be resolved.

The term “pyrolytic” is derived from “pyrolysis,” which is thermal decomposition. Pyrolytic carbon is formed from the thermal decomposition of hydrocarbons such as propane, propylene, acetylene, and methane, in the absence of oxygen. Without oxygen the typical decomposition of the hydrocarbon to carbon dioxide and water cannot take place; instead a more complex cascade of decomposition products occurs that ultimately results in a “polymerization” of the individual carbon atoms into large macroatomic arrays.

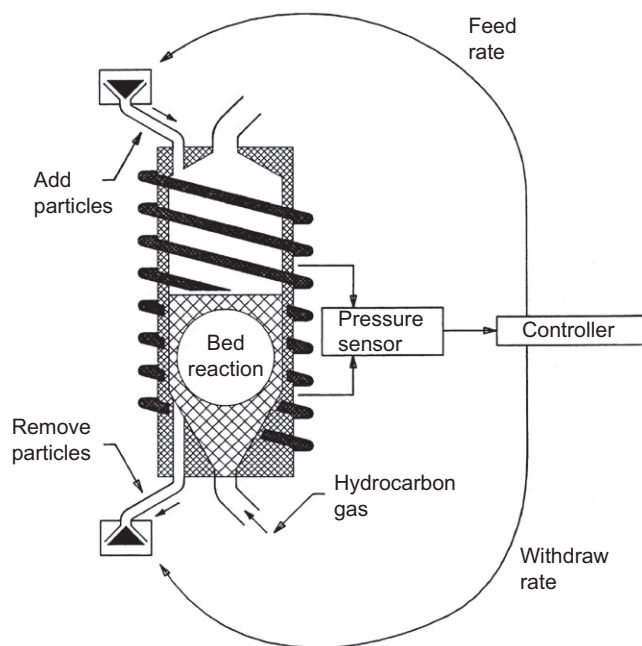


FIGURE 1.2.8.2 Fluidized-bed reactor schematic.

Pyrolysis of the hydrocarbon is normally carried out in a fluidized-bed reactor such as the one shown in Figure 1.2.8.2. A fluidized-bed reactor typically consists of a vertical tube furnace that may be induction or resistance heated to temperatures of 1000 to 2000°C (Bokros, 1969). Reactor diameters ranging from 2 cm to 25 cm have been used; however, the most common size used for medical devices has a diameter of about 10 cm. These high-temperature reactors are expensive to operate, and the reactor size limits the size of device components able to be produced.

Small refractory ceramic particles are placed into the vertical tube furnace. When a gas is introduced into the bottom of the tube furnace, the gas causes the particle bed to expand. Interparticle spacing increases to allow for the flow of the gas. Particle mixing occurs and the bed of particles begins to “flow” like a fluid. Hence the term “fluidized bed.” Depending upon the gas flow rate and volume, this expansion and mixing can be varied from a gentle bubbling bed to a violent spouting bed. An oxygen-free, inert gas, such as nitrogen or helium, is used to fluidize the bed, and the source hydrocarbon is added to the gas stream when needed.

At a sufficiently high temperature, pyrolysis or thermal decomposition of the hydrocarbon can take place. Pyrolysis products range from free carbon and gaseous hydrogen to a mixture of $C_x H_y$ decomposition species. The pyrolysis reaction is complex and is affected by the gas flow rate, composition, temperature, and bed surface area. Decomposition products, under the appropriate conditions, can form gas-phase nucleated droplets of carbon/hydrogen, which condense and deposit on the surfaces of the wall and bed particles within the reactor (Bokros, 1969). Indeed, the fluidized-bed process was

originally developed to coat small (200–500 micrometer) diameter spherical particles of uranium/thorium carbide or oxide with pyrolytic carbon. These coated particles were used as the fuel in the high temperature gas-cooled nuclear reactor (Bokros, 1969).

Pyrolytic carbon coatings produced in vertical tube reactors can have a variety of structures, such as laminar or isotropic, granular or columnar (Bokros, 1969). The structure of the coating is controlled by the gas flow rate (residence time in the bed), hydrocarbon species, temperature, and bed surface area. For example, an inadequately fluidized or static bed will produce a highly anisotropic, laminar pyrolytic carbon (Bokros, 1969).

Control of the first three parameters (gas flow rate, hydrocarbon species, and temperature) is relatively easy. However, until recently, it was not possible to measure the bed surface area while the reactions were taking place. As carbon deposits on the particles in the fluidized bed, the diameter of the particles increases. Hence the surface area of the bed changes, which in turn influences the subsequent rate of carbon deposition. As surface area increases, the coating rate decreases, since a larger surface area now has to be coated with the same amount of carbon available. Thus, the process is not in equilibrium. The static-bed process was adequate to coat nuclear fuel particles without attempting to control the bed surface area because such thin coatings (25–50 μm thick) did not appreciably affect the bed surface area.

It was later found that larger objects could be suspended within the fluidized bed of small ceramic particles and also become uniformly coated with carbon. This finding led to the demand for thicker, structural coatings, an order of magnitude thicker (250–500 μm). Bed surface area control and stabilization became an important factor (Akins and Bokros, 1974) in achieving the goal of thicker, structural coatings. In particular, with the discovery of the blood-compatible properties of pyrolytic carbon (LaGrange et al., 1969), thicker structural coatings with consistent and uniform mechanical properties were needed to realize the application to mechanical heart valve components. Quasi-steady-state conditions as needed to prolong the coating reaction were achieved empirically by removing coated particles and adding uncoated particles to the bed while the pyrolysis reaction was taking place (Akins and Bokros, 1974). However, the rates of particle addition and removal were based upon little more than good guesses.

Three of the four parameters that control carbon deposition could be accurately measured and controlled, but a method to measure and control bed surface area was lacking. Thus, the quasi-steady-state process was more of an art than a science. If too many coated particles were removed, the bed became too small to support the larger components within it and the bed collapsed. If too few particles were removed, the rate of deposition decreased, and the desired amount of coating was not achieved in the anticipated time. Furthermore, there

were considerable variations in the mechanical properties of the coating from batch to batch. It was found that in order to consistently achieve the hardness needed for wear resistance in prosthetic heart valve applications, it was necessary to add a small amount of β -silicon carbide to the carbon coating. The dispersed silicon carbide particles within the pyrolytic carbon matrix added sufficient hardness to compensate for potential variations in the properties of the pyrolytic carbon matrix. The β -silicon carbide was obtained from the pyrolysis of methyl-trichlorosilane, CH_3SiCl_3 . For each mole of silicon carbide produced, the pyrolysis of methyltrichlorosilane also produces three moles of hydrogen chloride gas. Handling and neutralization of this corrosive gas added substantial complexity and cost to an already complex process. Nevertheless, this process allowed consistency for the successful production of several million components for use in mechanical heart valves.

A process has been developed and patented that allows precise measurement and control of the bed surface area. A description of this process is given in the patent literature and elsewhere (Emken et al., 1993, 1994; Ely et al., 1998). With precise control of the bed surface area, it is no longer necessary to include the silicon carbide. Elimination of the silicon carbide has produced a stronger, tougher, and more deformable pure pyrolytic carbon. Historically, pure carbon was the original

objective of the development program because of the potential for superior biocompatibility (LaGrange et al., 1969). Furthermore, the enhanced mechanical and physical properties of the pure pyrolytic carbon now possible with the improved process control allow prosthesis design improvements in the hemodynamic contribution to thromboresistance (Ely et al., 1998).

Structure of Pyrolytic Carbons

X-ray diffraction patterns of the biomedical-grade fluidized-bed pyrolytic carbons are broad and diffuse because of the small crystallite size and imperfections. In silicon-alloyed pyrolytic carbon, a diffraction pattern characteristic of the β form of silicon carbide also appears in the diffraction pattern along with the carbon bands. The carbon diffraction pattern indicates a turbostratic structure (Kaae and Wall, 1996) in which there is order within carbon layer planes, as in graphite; but, unlike graphite, there is no order between planes. This type of turbostratic structure is shown in Figure I.2.8.3 compared to that of graphite. In the disordered crystalline structure, there may be lattice vacancies and the layer planes are curved or kinked. The ability of the graphite layer planes to slip is inhibited, which greatly increases the strength and hardness of the pyrolytic carbon relative to that of graphite. From the Bragg

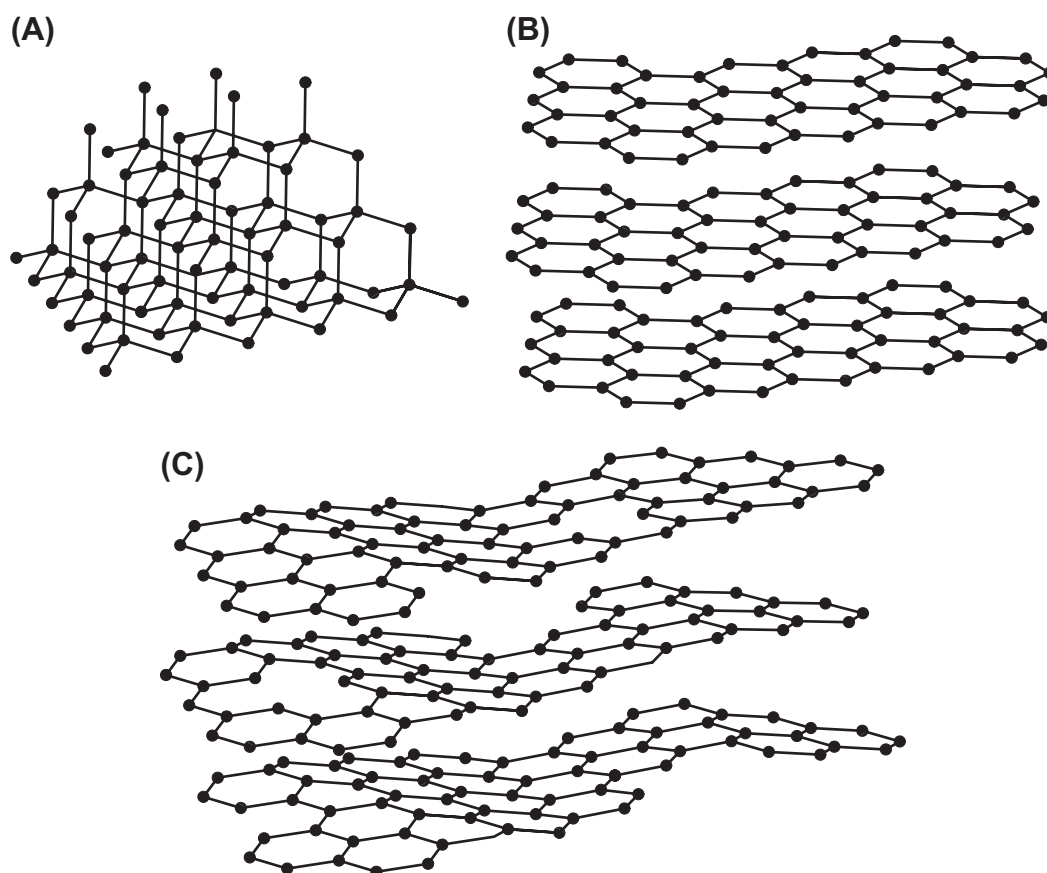


FIGURE I.2.8.3 Structures of: (A) diamond; (B) graphite; and (C) turbostratic pyrolytic carbon.

equation, the pyrolytic carbon layer spacing is reported to be 3.48 Å, which is larger than the 3.35 Å graphite layer spacing (Kaae and Wall, 1996). The increase in layer spacing relative to graphite is due to both the layer distortion and the small crystallite size, and is a common feature for turbostratic carbons. From the Scherrer equation the crystallite size is typically 25–40 Å (Kaae and Wall, 1996).

During the coating reaction, gas-phase nucleated droplets of carbon/hydrogen form that condense and deposit on the surfaces of the reactor wall and bed particles within the reactor. These droplets aggregate, grow, and form the coating. When viewed with high-resolution transmission electron microscopy, a multitude of

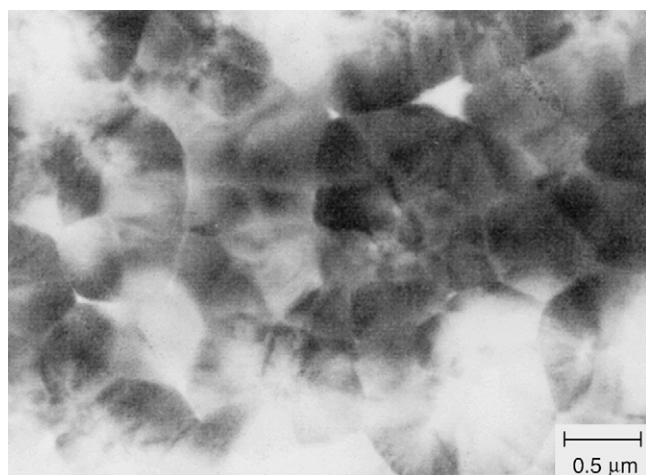


FIGURE 1.2.8.4 Electron micrograph of pure pyrolytic carbon microstructure showing near-spherical polycrystalline growth features formed during deposition (Kaae and Wall, 1996).

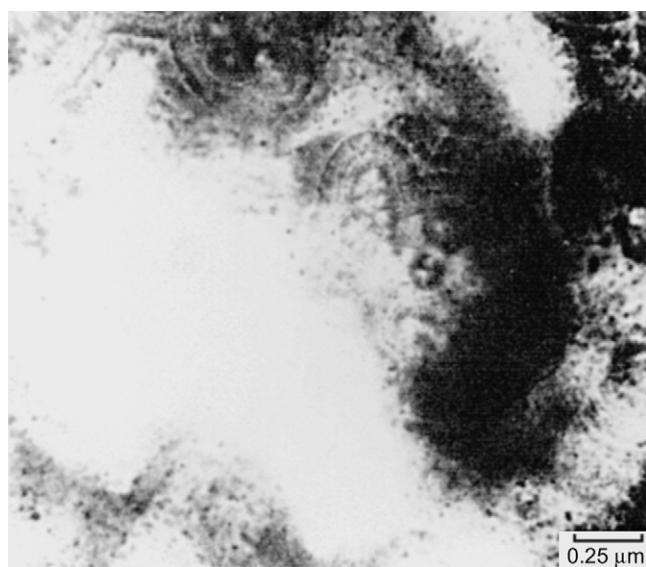


FIGURE 1.2.8.5 Electron micrograph of silicon-alloyed pyrolytic carbon microstructure showing near-spherical polycrystalline growth features formed during deposition (Kaae and Wall, 1996). Small silicon carbide particles are shown in concentric rings in the growth features.

near-spherical polycrystalline growth features are evident, as shown in Figure 1.2.8.4 (Kaae and Wall, 1996). These growth features are considered to be the basic building blocks of the material, and the shape and size are related to the deposition mechanism. In the silicon-alloyed carbon, small silicon carbide particles are present within the growth features, as shown in Figure 1.2.8.5. Based on a crystallite size of 33 Å, each growth feature contains about 3×10^9 crystallites. Although the material is quasi-crystalline on a fine level, the crystallites are very small and randomly oriented in the fluidized bed pyrolytic carbons so that overall the material exhibits isotropic behavior.

Glassy carbon, also known as vitreous carbon or polymeric carbon, is another turbostratic carbon form that has been proposed for use in long-term implants. However, its strength is low and the wear resistance is poor. Glassy carbons are quasi-crystalline in structure, and are named “glassy” because the fracture surfaces closely resemble those of glass (Haubold et al., 1981).

Vapor-deposited carbons are also used in heart valve applications. Typically, the coatings are thin ($<1 \mu\text{m}$) and may be applied to a variety of materials in order to confer the biochemical characteristics of turbostratic carbon. Some examples are vapor-deposited carbon coatings on heart valve sewing cuffs and metallic orifice components (Haubold et al., 1981).

Mechanical Properties

Mechanical properties of pure pyrolytic carbon, silicon-alloyed pyrolytic carbons, and glassy carbon are given in Table 1.2.8.1. Pyrolytic carbon flexural strength is

TABLE 1.2.8.1 Mechanical Properties of Biomedical Carbons

Property	Pure PyC	Typical Si-alloyed PyC	Typical Glassy Carbon
Flexural strength (MPa)	493.7 ± 12	407.7 ± 14.1	175
Young's modulus (GPa)	29.4 ± 0.4	30.5 ± 0.65	21
Strain-to-failure (%)	1.58 ± 0.03	1.28 ± 0.03	-
Fracture toughness (MPa $\sqrt{\text{m}}$)	1.68 ± 0.05	1.17 ± 0.17	0.5–0.7
Hardness (DPH, 500 g load)	235.9 ± 3.3	287 ± 10	150
Density (g/cm ³)	1.93 ± 0.01	2.12 ± 0.01	<1.54
CTE (10 ⁻⁶ cm/cm°C)	6.5	6.1	-
Silicon content (%)	0	6.58 ± 0.32	0
Wear resistance	Excellent	Excellent	Poor

high enough to provide the necessary structural stability for a variety of implant applications, and the density is low enough to allow for components to move easily under the applied forces of circulating blood. With respect to orthopedic applications, Young's modulus is in the range reported for bone (Reilly and Burstein, 1974; Reilly et al., 1974), which allows for compliance matching. Relative to metals and polymers, the pyrolytic carbon strain-to-failure rate is low; it is a nearly ideal linear elastic material and requires consideration of brittle material principles in component design. Strength levels vary with the effective stressed volume or stressed area, as predicted by classical Weibull statistics (De Salvo, 1970). The flexural strengths cited in Table I.2.8.1 are for specimens tested in four-point bending, third-point loading (More et al., 1993) with effective stressed volumes of 1.93 mm³. The pyrolytic carbon material Weibull modulus is approximately 10 (More et al., 1993).

Fracture toughness levels reflect the brittle nature of the material, but the fluidized-bed isotropic pyrolytic carbons are remarkably fatigue resistant. Recent fatigue studies indicate the existence of a fatigue threshold that is very nearly the single-cycle fracture strength (Gilpin et al., 1993; Ma and Sines, 1996, 1999, 2000). Fatigue-crack propagation studies indicate very high Paris-law fatigue exponents, on the order of 80, and display clear evidence of a fatigue-crack propagation threshold (Ritchie et al., 1990; Beavan et al., 1993; Cao, 1996).

Crystallographic mechanisms for fatigue-crack initiation, as occur in metals, do not exist in the pyrolytic carbons (Haubold et al., 1981). In properly designed and manufactured components, and in the absence of externally induced damage, fatigue does not occur in pyrolytic-carbon mechanical heart valve components. In the 30 years of clinical experience, there have been no clear instances of fatigue failure. Few pyrolytic carbon component fractures have occurred, less than 60 out of more than four million implanted components (Haubold, 1994), and most are attributable to induced damage from handling or cavitation (Kelpetko et al., 1989; Kafesjian et al., 1994; Richard and Cao, 1996).

Wear resistance of the fluidized-bed pyrolytic carbons is excellent. The strength, stability, and durability of pyrolytic carbon are responsible for the extension of mechanical valve lifetimes from less than 20 years to more than the recipient's expected lifetime (Schoen et al., 1982; Schoen, 1983; More and Silver, 1990; Wieting, 1996).

Pyrolytic carbon in heart valve prostheses is often used in contact with metals, either as a carbon disk in a metallic valve orifice or as a carbon orifice stiffened with a metallic ring. Carbon falls with the noble metals in the galvanic series (Haubold et al., 1981), the sequence being silver, titanium, graphite, gold, and platinum. Carbon can accelerate corrosion when

coupled to less noble metals *in vivo*. However, testing using mixed potential corrosion theory and potentiostatic polarization has determined that no detrimental effects occur when carbon is coupled with titanium or cobalt–chrome alloys (Thompson et al., 1979; Griffin et al., 1983). Carbon couples with stainless steel alloys are not recommended.

STEPS IN THE FABRICATION OF PYROLYTIC CARBON COMPONENTS

To convert a gaseous hydrocarbon into a shiny, polished black component for use in the biological environment is not a trivial undertaking. Furthermore, because of the critical importance of long-term implants to a recipient's health, all manufacturing operations are performed to stringent levels of quality assurance under the auspices of US Food and Drug Administration Good Manufacturing Practices and International Standards Organization ISO-9000 regulations. As in the case of fabrication of metallic implants, numerous steps are involved. Pyrolytic carbon is not machined from a block of material, as is the case with most metallic implants, nor is it injection or reactive molded, as are many polymeric devices. An overview of the processing steps leading to a finished pyrolytic carbon coated component for use in a medical device is shown in Figure I.2.8.6, and is further described in the following sections.

Substrate Material

Since pyrolytic carbon is a coating, it must be deposited on an appropriately shaped, preformed substrate (preform). Because the pyrolysis process takes place at high temperatures, the choice of substrates is severely

Steps in the fabrication of pyrolytic carbon components

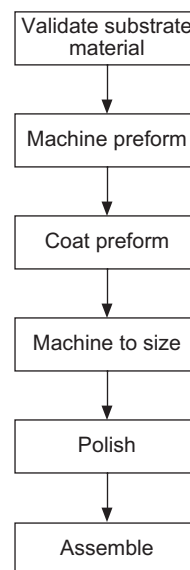


FIGURE I.2.8.6 Schematic of manufacturing processing steps.

limited. Only a few of the refractory materials, such as tantalum or molybdenum/rhenium alloys and graphite, can withstand the conditions at which the pyrolytic carbon coating is produced. Some refractory metals have been used in heart valve components; for example, Mo/Re preforms were coated to make the struts for the Beall–Surgitool mitral valve. It is important for the thermal expansion characteristics of the substrate to closely match those of the applied coating. Otherwise, upon cooling of the coated part to room temperature the coating will be highly stressed and can spontaneously crack. For contemporary heart valve applications, fine-grained isotropic graphite is the most commonly used substrate. This substrate graphite can be doped with tungsten in order to provide radioopacity for X-ray visualizations of the implants. The graphite substrate does not impart structural strength. Rather, it provides a dimensionally stable platform for the pyrolytic carbon coating, both at the reaction temperature and at room temperature.

Preform

Once the appropriate substrate material has been selected and prior to making a preform, it must be inspected to ensure that the material meets the desired specifications. Typically, the strength and density of the starting material are measured. Thermal expansion is ordinarily validated and monitored through process control. The preform, which is an undersized replica of the finished component, is normally machined using conventional machining methods. Because the fine-grained isotropic graphite is very abrasive, standard machine tools have given way to diamond-plated or single-point diamond tools. In the case of heart valves, numerical control machining methods are often required to maintain critical component dimensional tolerances. After the preform is completed, it is inspected to ensure that its dimensions fall within the specified tolerances and that it contains no visible flaws or voids.

Coating

Generally numerous preforms are coated in one furnace run. A batch to be coated is made up of substrates from a single lot of preforms. Such batch processing by lot is required in order to maintain “forward and backward” traceability. In other words, ultimately it is necessary to know all of the components that were prepared using a specific material lot, given either the starting material lot number (forward) or given the specific component serial number (backward). The number of parts that can be coated in one furnace run is dictated by the size of the furnace and the size and weight of the parts to be coated. The batch of substrates is placed within the fluidized bed in the vertical tube furnace and is coated to the desired thickness. Coating times are generally on the order of

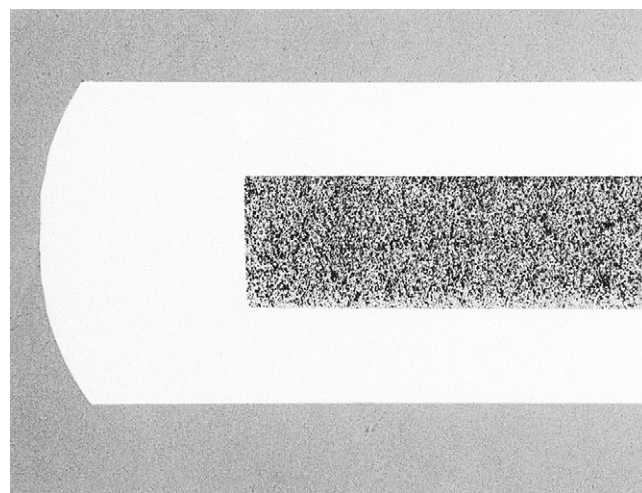


FIGURE 1.2.8.7 Metallographic mount cross-section of heat valve component. The light-colored pyrolytic carbon layer is coated over the interior, darker-colored granular-appearing graphite substrate.

a few hours, but the entire cycle (heat-up, coating, and cool-down) may take as long as a full day.

A statistical sample from each coating lot is taken for analysis. At this point, typical measurements include coating thickness, microhardness, and microstructure. The microhardness and microstructure are determined from a metallographically prepared cross-section of the coated component taken perpendicular to the plane of deposition. Thus, this test is destructive. An example of a metallographically prepared cross-section of a pyrolytic carbon component is shown in [Figure 1.2.8.7](#).

Machine to Size

The components used to manufacture medical devices have strict dimensional requirements. Because of the inability, until recently, to precisely measure and control bed size, and indirectly coating thickness, the preforms were generally coated more thickly than necessary to ensure adequate pyrolytic carbon coating thickness on the finished part. The strict dimensional requirements were then achieved through precision grinding or other machining operations. Because pyrolytic carbon is very hard, conventional machine tools again cannot be used. Diamond-plated grinding wheels and other diamond tooling are required. The dimensions of final machined parts are again verified.

Polish

The surface of as-deposited, machined, and polished components is shown in [Figure 1.2.8.8](#). It was found early on in experiments ([LaGrange et al., 1969](#); [Sawyer et al., 1975](#); [Haubold et al., 1981](#)) that clean polished pyrolytic carbon surfaces of tubes when placed within the vasculature of experimental animals accumulated minimal if any thrombus; and certainly less than

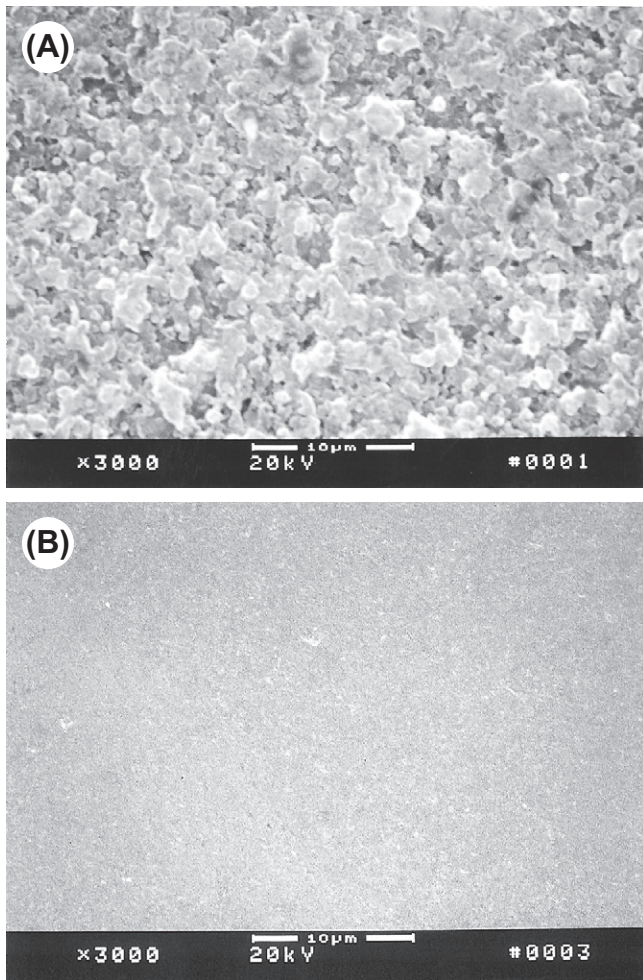


FIGURE 1.2.8.8 Scanning electron microscope micrographs of: (A) as-coated; and (B) as-polished surfaces.

pyrolytic carbon tubes with the as-deposited surface. Consequently, the surfaces of pyrolytic carbon have historically been polished, either manually or mechanically, using fine diamond or aluminum oxide pastes and slurries. The surface finish achieved has roughness measured on the scale of nanometers. As can be seen from Table 1.2.8.2 (More and Haubold, 1996), the surfaces of polished pyrolytic carbon (30–50 nm) are an order of magnitude smoother than the as-deposited surfaces (300–500 nm).

Once the desired surface quality is achieved, components are again inspected. The final component inspection may include measurement of dimensions, X-ray inspection in two orientations to verify coating thickness, and visual inspection for surface quality and flaws. In many cases, automated inspection methods with computer-controlled coordinate measurement machines are used. X-ray inspection can be used to ensure that minimum coating thickness requirements are met. Two orthogonal views ensure that machining and grinding of the coating was achieved uniformly, and that the coating is symmetrical. The machining and grinding operation after coating is not without the risk of inducing cracks

TABLE 1.2.8.2

Surface Finish (R_a , Average, and R_q , Root Mean Square) of Pyrolytic Carbon Heat Valve Components^a

Specimen	R_a (nm)	R_q (nm)	Comments
Glass microscope slide	17.14	26.80	
On-X leaflet	33.95	42.12	Clinical
Sorin Bicarbon leaflet	40.12	50.63	Nonclinical
SJM leaflet	49.71	62.74	Clinical
CMI (SJM) leaflet	67.98	85.56	Nonclinical
Sorin Monoleaflet	99.59	128.10	Clinical
DeBakey–Surgitool ball	129.78	157.93	Nonclinical
As-coated slab	389.07	503.72	

^aComponents/prepared by: On-X/Medical Carbon Research Institute, Austin, TX, USA; Sorin/Sorin Biomedica, Saluggia, Italy; SJM/Saint Jude Medical, Saint Paul, MN, USA; CMI (SJM)/CarboMedics, Austin, TX, USA; DeBakey-S/CarboMedics, San Diego, USA (circa 1968). “Clinical” was from as-packaged valve; “nonclinical” lacks component traceability.

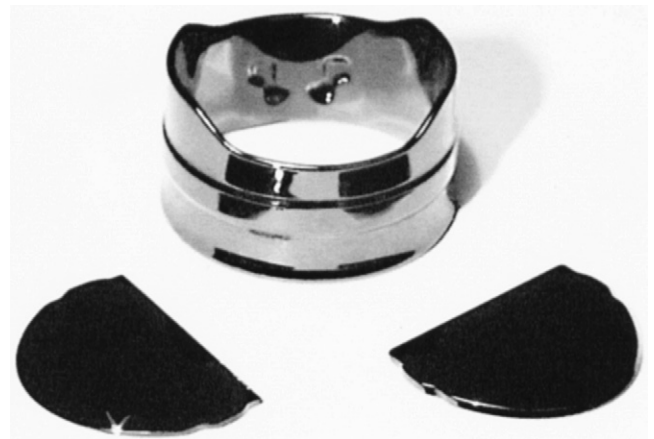


FIGURE 1.2.8.9 Components for On-X bileaflet heart valve.

or flaws in the coating, which may subsequently affect the service life of the component. Such surface flaws are detected visually or with the aid of dye-penetrant techniques. Components may also be proof-tested to detect and eliminate components with subsurface flaws. With the advent of bed size control, which allows coating to exact final dimensions, the concerns about flaws introduced during the machining and grinding operation have been eliminated.

The polished and inspected components, thus prepared, are now ready for assembly into devices, or are packaged and sterilized in the case of standalone devices. Shown in Figure 1.2.8.9 are the three pyrolytic carbon components for a bileaflet mechanical heart valve. The components were selected and matched for assembly using the data generated from the final dimensional inspection to achieve the dimensional requirements specified in the device design. In Figure 1.2.8.10, the pyrolytic carbon components for a



FIGURE 1.2.8.10 Replacement metacarpophalangeal total joint prosthesis components, Ascension Orthopedics, Austin TX, USA.

replacement metacarpophalangeal total joint prostheses are shown.

Assembly

The multiple components of a mechanical heart must be assembled. The brittleness of pyrolytic carbon poses a significant assembly problem. Because the strain-to-failure is on the order of 1.28% to 1.58%, there is a limited range of deformation that can be applied in order to achieve a proper fit. Relative fit between the components defines the capture and the range of motion for components that move to actuate valve opening and closing. Furthermore, component obstructive bulk and tolerance gaps are critical to hemodynamic performance.

In designs that use a metallic orifice, the metallic components are typically deformed in order to insert the pyrolytic carbon occluder disk. For the all-carbon bileaflet designs, the carbon orifice must be deflected in order to insert the leaflets. As the valve diameter decreases, and as the section modulus of the orifice design increases, the orifice stiffness increases. The possibility of damage or fracture during assembly was a limiting factor in early orifice design. For this reason, the orifices in valve designs using silicon-alloyed pyrolytic carbon were simple cylindrical geometries, and the smallest sizes were limited to the equivalent of a 19 mm diameter tissue annulus. The simple cylindrical orifice designs are often reinforced with a metallic stiffening ring that is shrunk on after assembly. The stiffening ring ensures that physiological loading will not produce deflections that can inhibit valve action or result in leaflet escape.

The increased strain-to-failure of pure pyrolytic carbon, relative to the silicon-alloyed carbon, allows designs with more complex orifice section moduli. This allows designers to utilize hydrodynamically efficient shapes such as flared inlets and to incorporate external stiffening bands that eliminate the need for a metallic stiffening ring. The increased strain-to-failure of On-X carbon has been used to advantage in the On-X mechanical heart valve design (Ely et al., 1998).

Cleaning and Surface Chemistry

Pyrolytic carbon surface chemistry is important because the manufacturing and cleaning operations to which a component is subjected can change and redefine the surface that is presented to the blood. Oxidation of carbon surfaces can produce surface contamination that detracts from blood compatibility (LaGrange et al., 1969; Bokros et al., 1969). Historically, the initial examinations of pyrolytic carbon biocompatibility assumed *de facto* that the surface needed to be treated with a thromboresistant agent such as heparin (Bokros et al., 1969). It was found, however, that the non-heparin-coated surface was actually more blood compatible than the treated surface. Hence, the efforts toward surface coating with heparin were abandoned.

In general it is desired to minimize the surface oxygen and any other non-carbon surface contaminants. From X-ray photoelectron spectroscopy (XPS) analyses, a typical heart valve component surface has 76–86% C, 12–21% O, 0–2% Si, and 1–2% Al (King et al., 1981; Smith and Black, 1984; More and Haubold, 1996). Polishing compounds tend to contain alumina, and some alumina particles may become imbedded in the carbon surface. Other contaminants that may be introduced at low levels (<2% each) are Na, B, Cl, S, Mg, Ca, Zn, and N. The XPS carbon 1s peak when scanned at high resolution can be deconvoluted to determine carbon oxidation states. The carbon 1s peak will typically consist primarily of hydrocarbon-like carbon (60–81%), ether alcohol/ester-like carbon (10–24%), ketone-like carbon (0–6%), and ester/acid-like carbon (1–12%) (More and Haubold, 1996). Each manufacturing, cleaning, and sterilizing operation potentially redefines the surface. The effect of modified surface chemistry on blood compatibility is not well characterized, so this adds a level of uncontrolled variability when considering the blood compatibility of pyrolytic-carbon heart valve materials from different manufacturing sources and different investigators. In general, the presence of oxygen and surface contaminants should be eliminated.

BIOCOMPATIBILITY OF PYROLYTIC CARBON

The suitability of a material for use in an implant is a complex issue. Biocompatibility testing is the focus of other chapters. In the case of pyrolytic carbon, its successful history interfacing with blood in mechanical heart valves attests to its suitability for this application. A note of caution, however, is in order. Until about a decade ago, the pyrolytic carbon used so successfully in mechanical heart valves was produced by a single manufacturer; the material, many applications in the biological environment, and the processes for producing the material, were all patented. Since the expiration of the last of these patents in 1989, other sources for pyrolytic carbon have

appeared that are copies of the original General Atomic material. When considering alternative carbon materials, it is important to recognize that the proper combination of physical, mechanical, and blood-compatible properties is required for the success of the implant application. Furthermore, because there are a number of different possible pyrolysis processes, it should be recognized that each can result in different microstructures with different properties. Just because a material is carbon, a turbostratic carbon or a pyrolytic carbon does not qualify its use in a long-term human implant (Haubold and Ely, 1995). For example, pyrolytic carbons prepared by chemical vapor deposition processes, other than the fluidized-bed process, are known to exhibit anisotropy, nonhomogeneity, and considerable variability in mechanical properties (Agafonov et al., 1999). Although these materials may exhibit biocompatibility, the potential for variability in structural stability and durability may lead to valve dysfunction.

The original General Atomic-type fluidized-bed pyrolytic carbons all demonstrate negligible reactions in the standard Tripartite and ISO 10993-1 type biocompatibility tests. Results from such tests are given in Table I.2.8.3 (Ely et al., 1998). Pure pyrolytic carbon is so non-reactive that it can serve as a negative control for these tests.

It is believed that pyrolytic carbon owes its demonstrated blood compatibility to its inertness and to its ability to quickly absorb proteins from blood without triggering a protein denaturing reaction. Ultimately, the blood compatibility is thought to be a result of the protein layer formed upon the carbon surface. Baier observed that pyrolytic carbon surfaces have a relatively high critical surface tension of 50 dyn/cm, which immediately drops to 28–30 dyn/cm following exposure to blood (Baier et al., 1970). The quantity of sorbed protein was thought to be an important factor for blood compatibility. Lee and Kim (1974) quantified the amount of radiolabeled proteins sorbed from solutions of mixture proteins (albumin, fibrinogen, and gamma-globulin). While pyrolytic carbon does adsorb albumin, it also adsorbs a considerable quantity of fibrinogen, as shown in Figure I.2.8.11. As can be seen in Figure I.2.8.11, the amount of fibrinogen adsorbed on pyrolytic carbon surfaces is far greater than the amount of albumin on these surfaces, and is comparable to the amount of fibrinogen that is sorbed on silicone rubber. The mode of albumin adsorption, however, appears to be drastically different for these two materials. Albumin sorbs immediately on the pyrolytic carbon surfaces, whereas the build-up of fibrinogen is much slower. In the case of silicone rubber, both proteins sorb at a much slower rate. It appears that

TABLE I.2.8.3 Biological Testing of Pure PyC

Test Description	Protocol	Results
Klingman maximization	ISO/CD 10993–10	Grade 1; not significant
Rabbit pyrogen	ISO/DIS 10993–11	Nonpyrogenic
Intracutaneous injection	ISO 10993–10	Negligible irritant
Systemic injection	ANSI/AAMI/ISO 10993–11	Negative – same as controls
<i>Salmonella typhimurium</i> reverse mutation assay	ISO 10993–3	Nonmutagenic
Physico-chemical	USP XXIII, 1995	Exceeds standards
Hemolysis – rabbit blood	ISO 10993–4/NIH 77–1294	Nonhemolytic
Elution test (L929 mammalian cell culture)	ISO 10993–5, USP XXIII, 1995	Noncytotoxic

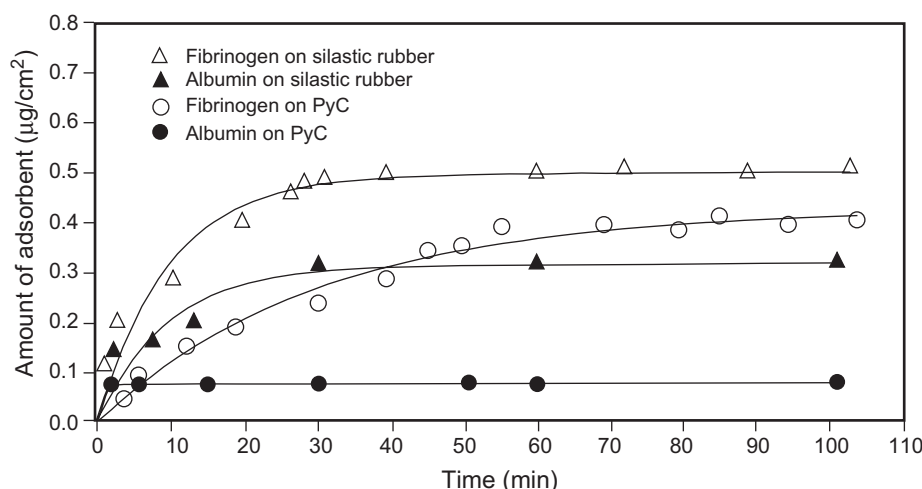


FIGURE I.2.8.11 Fibrinogen and albumin adsorption on pyrolytic carbon (PyC) and Silastic silicone rubber.

the mode of protein adsorption is important, and not the total amount sorbed.

Nyilas and Chiu (1978) studied the interaction of plasma proteins with foreign surfaces by measuring directly the heats of adsorption of selected proteins onto such surfaces using microcalorimetric techniques. They found that the heats of adsorption of fibrinogen, up to the completion of first monolayer coverage, are a factor of eight smaller on pyrolytic carbon surfaces than on the known thrombogenic control (glass) surface, as shown in Figure I.2.8.12. Furthermore, the measured net heats of adsorption of gamma globulin on pyrolytic carbon were about 15 times smaller than those on glass. They concluded that low heats of adsorption onto a foreign surface imply small interaction forces with no conformational changes of the proteins that might trigger the clotting cascade. It appears that a layer of continuously exchanging blood proteins in their unaltered state “masks” the pyrolytic carbon surfaces from appearing as a foreign body.

There is further evidence that the minimally altered sorbed protein layers on pyrolytic carbon condition blood compatibility. Salzman et al. (1977), for example, observed a significant difference in platelet reaction with pyrolytic carbon beads in packed columns prior to and after pretreatment with albumin. With no albumin preconditioning treatment, platelet retention by the columns was high, but the release of platelet constituents was low. However, with albumin pretreatment, platelet retention and the release of constituents was minimal.

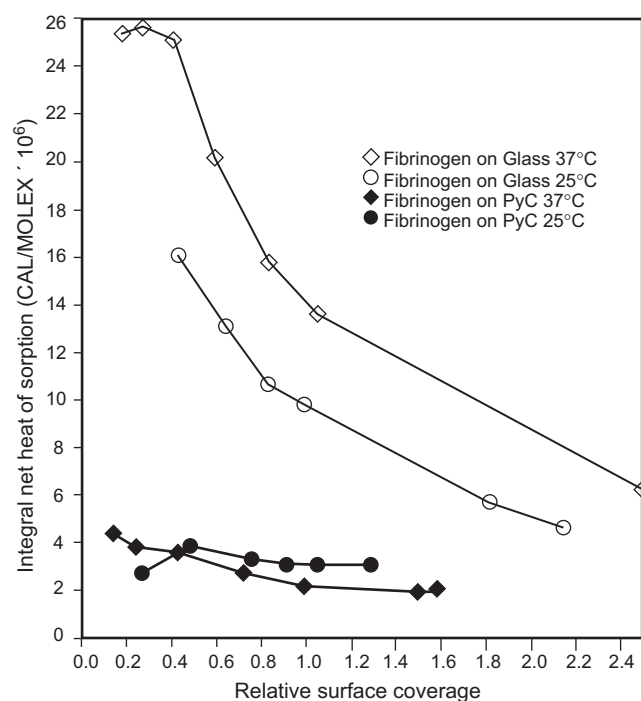


FIGURE I.2.8.12 Integral heat of sorption for fibrinogen on glass and fibrinogen on PyC at two different temperatures (Nyilas and Chiu, 1978).

The foregoing observations led to the view that pyrolytic carbon owes its demonstrated blood compatibility to its inertness, and to its ability to quickly adsorb proteins from blood without triggering a protein-denaturing reaction (Nyilas and Chiu, 1978; Haubold et al., 1981). However, the assertion that pyrolytic carbon is an inert material and induces minimal conformational changes in adsorbed protein was re-examined by Feng and Andrade (1994). Using differential scanning calorimetry and a variety of proteins and buffers, they found that pyrolytic carbon surfaces denatured all of the proteins studied. They concluded that whether or not a surface denatures protein cannot be the sole criteria for blood compatibility. Their suggestion was that the specific proteins and the sequence in which they are denatured may be important. For example, it was suggested that pyrolytic carbon may first adsorb and denature albumin, which forms a layer that subsequently passivates the surface and inhibits thrombosis.

Chinn et al. (1994) re-examined the adsorption of albumin and fibrinogen on pyrolytic carbon surfaces and noted that relatively large amounts of fibrinogen were adsorbed, and speculated that the adsorbed fibrinogen was rapidly converted to a non-elutable form. If the elutable form is more reactive to platelets than the non-elutable form, then the non-elutable protein layer may contribute to the passivating effect.

Work on visualizing the carbon surface and platelet adhesion done by Goodman et al. (1995) using low accelerating-voltage scanning electron microscopy, along with critical-point drying techniques, has discovered that the platelet spreading on pyrolytic carbon surfaces is more extensive than previously observed (Haubold et al., 1981). However, platelet loading was in a static flow situation that does not model the physiological flow that a heart valve is subjected to. Hence, this approach cannot resolve kinetic effects on platelet adhesion. However, Okazaki, Tweden, and co-workers observed adherent platelets on valves following implantation in sheep that were not treated with anticoagulants (Okazaki et al., 1997). There were no instances of valve thrombosis, even though platelets were present on some of the valve surfaces. But the relevance of this observation to clinical valve thromboses is not clear, because human patients with mechanical heart valves undergo chronic anticoagulant therapy (Edmunds, 1987), and have a hemostatic system different from that of sheep.

A more contemporary version of the mechanism of pyrolytic carbon blood compatibility might be to reject the assumption that the surface is inert, as it is now thought by some that no material is totally inert in the body (Williams, 1998), and to accept that the blood-material interaction is preceded by a complex, interdependent, and time-dependent series of interactions between the plasma proteins and the surface (Hanson, 1998) that is as yet poorly understood. To add to the confusion, it must also be recognized that much of the

forementioned conjecture depends on the assumption that all of the carbon surfaces studied were in fact pure and comparable to one another.

CLINICAL APPLICATIONS

Widespread clinical use of pyrolytic carbon components for heart valve replacement began in October of 1968 when Dr. Michael DeBakey implanted an aortic valve with a hollow Pyrolite® carbon ball occluder. Following this first implant, several million PyC mechanical valve prostheses have been implanted worldwide, generating an experience on the order of 20 million patient-years. Use of PyC to replace polymers in valve prostheses was declared an “exceptional event” (Sadeghi, 1987) because the superior durability, stability, and biocompatibility of PyC enabled valves to endure for the patient’s lifetime.

However, patients with mechanical valve prostheses require chronic anticoagulation therapy because of the risk of valve-related hemostatic complications. In efforts to reduce the risk of hemostatic complications and the need for chronic anticoagulation, it was hypothesized that valve-related hemostatic complications were in part due to flow-induced mechanical trauma to the blood, and to the presence of PyC itself because of the potential thrombogenicity of the silicon-carbide alloy constituent (LaGrange et al., 1969).

In 1992, advances in pyrolytic carbon manufacturing technology enabled precise control of processing parameters (Bokros et al., 1994). With this precise control it was possible to produce pure isotropic pyrolytic carbons having significantly improved properties relative to silicon-alloyed PyC, thus eliminating the need for the silicon-carbide alloy (see Table I.2.8.1). Precise process control also enabled a coat-to-size capability needed to eliminate surface blemishes caused by post-coating machining processes such as grinding.

The On-X valve shown in Figure I.2.8.9 was specifically designed to exploit the improved pure PyC which enables features to reduce flow-induced trauma (Bokros et al., 1994, 1997, 1998, 2003), and introduced into clinical practice (FDA, 2001, 2002). The success of the On-X valve in general clinical experience, particularly in noncompliant anticoagulant therapy patient populations (Williams and van Riet, 2006) and animal studies (Flameng and Meuris, 2002) strongly indicated improvements in mechanical valve-related hemostatic complications. Data from this experience was used to justify the first and only FDA approved non-warfarin and reduced warfarin prospective randomized trial for a mechanical heart valve. This trial for the On-X Prosthetic Heart Valve, with the objective to reduce anticoagulation bleeding risk, was initiated at Emory Crawford Long Hospital, Atlanta in 2006. The trial is currently ongoing at 40 institutions to include 1200 patients. The high risk aortic group has been fully enrolled, with more than 500 pt-yr experience, maintained with a reduced dose

of Coumadin (INR of 1.5 to 2.0) and aspirin (81 mg/dy). The low risk aortic group is maintained with platelet inhibitors, (75 mg/dy plavix) and aspirin. The mitral group enrollment was extended to 2012; this group is maintained at an INR of 2.0 to 2.5 and aspirin (81 mg/dy). A successful outcome for this trial would offer further improvements in quality of life for a significant number of On-X mechanical heart valve recipients.

During the past 28 years PyC has also been used as a loadbearing material for small orthopedic joint replacement implants. Such prostheses relieve pain, correct deformity, and improve the appearance of joints damaged by disease such as rheumatoid arthritis, osteoarthritis, and post-traumatic conditions. However, all PyC joint replacements require careful patient selection for good quality bone and soft tissue. As is true with all implants, prosthesis sizing, alignment, and interactions with soft tissue are critical considerations during implantation surgery and rehabilitation.

Successful applications for upper limb total joint prostheses include the metacarpophalangeal (MCP) joint (Figure I.2.8.10) and the proximal interphalangeal (PIP) joint (Cook et al., 1999; Bravo et al., 2007). Pure isotropic PyC is a nearly ideal material for orthopedic application, with demonstrated advantages over traditional materials such as polymers, ceramics, and metals (Stanley et al., 2008) which include:

- Elimination of wear-related failures
- Absence of osteolytic adverse tissue reactions
- Excellent fatigue resistance
- Non-cemented fixation via bone apposition
- Minimization of stress shielding effects and bone resorption
- Excellent compatibility with joint cartilage and bone tissues.

This excellent compatibility with cartilage and bone tissue enables a number of hemiarthroplasty applications, in which only one component of the joint is replaced leaving the PyC device bearing and articulating against native synovial surfaces. Successful devices for hemiarthroplasty include the MCP and PIP joints, carpometacarpal (CMC) joints, radial head, lunate, and inter-positional articulating surface spacers for use in the CMC joint. Currently, approximately 18,000 PyC small joint and hemiarthroplasty devices have been implanted worldwide.

Given the clinical success of the small joint implants, enhanced compatibility with joint tissue, superior durability, and potential significantly extended device lifetimes, efforts are currently underway to use PyC as a platform for larger joint implants such as the shoulder, knee, and hip. In the larger loadbearing joints, a viable strategy is to use PyC as the bearing surface in conservative resurfacing devices and in total joint modular devices. The mechanical valve experience has demonstrated excellent PyC compatibility with traditional

implant material metals, ceramics, and polymers. This PyC materials compatibility lends great versatility in design for modular devices. We fully expect that PyC devices will prove more functional, aesthetic, durable, and complication free than implants with traditional materials only.

CONCLUSION

Because the blood compatibility of pyrolytic carbon in mechanical heart valves is not perfect, anticoagulant therapy is required for mechanical heart valve patients. However, pyrolytic carbon has been the most successful material in heart valve applications because it offers excellent blood and tissue compatibility which, combined with the appropriate set of physical and mechanical properties and durability, allows for practical implant device design and manufacture. Improvements in biocompatibility are desired, of course, because when heart valves and other implants are used, a deadly or disabling disease is often treated by replacing it with a less pathological, more manageable chronic condition. Ideally, an implant should not lead to a chronic condition.

It is important to recognize that the mechanism for the blood compatibility of pyrolytic carbons is not fully understood, nor is the interplay between the bio-material itself, design-related hemodynamic stresses, and the ultimate biological reaction. The elucidation of the mechanism for blood and tissue compatibility of pyrolytic carbon remains a challenge.

It is also worth restating that the suitability of carbon materials from new sources for long-term implants is not assured simply because the material is carbon. Elemental carbon encompasses a broad spectrum of possible structures and mechanical properties. Each new candidate carbon material requires a specific assessment of biocompatibility based on its own merits, and not by reference to the historically successful General Atomic-type pyrolytic carbons.

BIBLIOGRAPHY

Agafonov, A., Kouznetsova, E., Kouznetsova, V., & Reif, T. (1999). TRI carbon strength and macroscopic isotropy of boron carbide alloyed pyrolytic carbon. *Artif. Organs*, 23(7), 80.

Akins, R. J., & Bokros, J. C. (1974). The deposition of pure and alloyed isotropic carbons and steady state fluidized beds. *Carbon*, 12, 439–452.

Baier, R. E., Gott, V. L., & Feruse, A. (1970). Surface chemical evaluation of thrombo-resistant materials before and after venous implantation. *Trans. Am. Soc. Artif. Intern. Organs*, 16, 50–57.

Beavan, L. A., James, D. W., & Kepner, J. L. (1993). Evaluation of Fatigue in Pyrolite Carbon. In P. Ducheyne, & D. Christiansen (Eds.), *Bioceramics* Vol. 6, (pp. 205–210). Oxford, UK: Butterworth-Heinemann.

Bokros, J. C. (1969). Deposition, Structure and Properties of Pyrolytic Carbon. In P. L. Walker (Ed.), *Chemistry and Physics of Carbon* Vol. 5, (pp. 1–118). New York, NY: Marcel Dekker.

Bokros, J. C., Gott, V. L., LaGrange, L. D., Fadall, A. M., Vos, K. D., et al. (1969). Correlations between blood compatibility and heparin adsorptivity for an impermeable isotropic pyrolytic carbon. *J. Biomed. Mater. Res.*, 3, 497–528.

Bokros, J. C., Emken, M. R., Haubold, A. D., et al. (1994). *Prosthetic heart valve*. US Patent No. 5,308,361: Issued May 3, 1994.

Bokros, J. C., Ely, J. L., Emken, M. R., et al. (1997). *Prosthetic heart valve*. US Patent No. 5,642,324: Issued June 24, 1997.

Bokros, J. C., Ely, J. L., Emken, M. R., et al. (1998). *Prosthetic heart valve with improved blood flow*. US Patent No. 5,772,694: Issued June 30, 1998.

Bokros, J. C., Stupka, J. C., More, R. B., et al. (2003). *Prosthetic heart valve*. US Patent No. 6,096,075: Issued August 1, 2003.

Bravo, C. J., Rizzo, R., Hormel, K. B., & Beckenbaugh, R. D. (2007). Pyrolytic carbon proximal interphalangeal joint arthroplasty: Results with minimum two-year follow-up evaluation. *J. Hand Surg.*, 32A, 1–11.

Cao, H. (1996). Mechanical performance of pyrolytic carbon in prosthetic heart valve applications. *J. Heart Valve Dis.*, 5(Suppl. I), S32–S49.

Chinn, J. A., Phillips, R. E., Lew, K. R., & Horbett, T. A. (1994). Fibrinogen and albumin adsorption to pyrolite carbon. *Trans. Soc. Biomater.*, 17, 250.

Cook, S. D., Beckenbaugh, R. D., Redondo, J., Popich, L. S., Klawitter, J. J., et al. (1999). Long term follow-up of pyrolytic carbon metacarpophalangeal implants. *J. Bone and Joint Surg.*, 81A(5), 635–648.

De Salvo, G. (1970). *Theory and Structural Design Applications of Weibull Statistics, Report WANL-TME-2688*, Westinghouse Electric Corporation.

Dillard, J. G. (1995). X-ray Photoelectron Spectroscopy (XPS) and Electron Spectroscopy for Chemical Analysis (ESCA). In H. Ishida, & L. E. Fitzpatrick (Eds.), *Characterization of Composite Materials* Vol. 1, (pp. 22). Boston, MA: Butterworth-Heinemann.

Edmunds, L. H. (1987). Thrombotic and bleeding complications of prosthetic heart valves. *Ann. Thorac. Surg.*, 44, 430–445.

Ely, J. L., Emken, M. R., Accuntius, J. A., Wilde, D. S., Haubold, A. D., et al. (1998). Pure pyrolytic carbon: Preparation and properties of a new material, on-X carbon for mechanical heart valve prostheses. *J. Heart Valve Dis.*, 7, 626–632.

Emken, M. R., Bokros, J. C., Accuntius, J. A., & Wilde, D. S. (1993). *Precise control of pyrolytic carbon coating*. Buffalo, New York: Presented at the 21st Biennial Conference on Carbon. June 13–18, 1993, Extended Abstracts and Program Proceedings, pp. 531–532.

Emken, M. R., Bokros, J. C., Accuntius, J. A., & Wilde, D. S. (1994). U.S. Patent No. 5,284,676, *Pyrolytic deposition in a fluidized bed*. Feb. 8, 1994.

Feng, L., & Andrade, J. D. (1994). Protein adsorption on low-temperature isotropic carbon: I. Protein conformational change probed by differential scanning calorimetry. *J. Biomed. Mater. Res.*, 28, 735–743.

Flameng, W., & Meuris, B. (2002). *Performance of bileaflet heart valve prostheses in an animal model of heart valve thrombosis*. 6th Annual Hilton Head Workshop on Prosthetic Heart Valves. South Carolina: Hilton Head. March 610.

Gilpin, C. B., Haubold, A. D., & Ely, J. L. (1993). Fatigue Crack Growth and Fracture of Pyrolytic Carbon Composites. In P. Ducheyne, & D. Christiansen (Eds.), *Bioceramics* Vol. 6, (pp. 217–223). Oxford, UK: Butterworth-Heinemann.

Goodman, S. L., Tweden, K. S., & Albrecht, R. M. (1995). Three-dimensional morphology and platelet adhesion on pyrolytic carbon heart valve materials. *Cells Mater.*, 5(1), 15–30.

Griffin, C. D., Buchanan, R. A., & Lemons, J. E. (1983). *In vitro* electrochemical corrosion study of coupled surgical implant materials. *J. Biomed. Mater. Res.*, 17, 489–500.

- Hanson, S. R. (1998). Blood–Material Interactions. In J. Black, & G. Hastings (Eds.), *Handbook of Biomaterial Properties* (pp. 545–555). London, UK: Chapman and Hall.
- Haubold, A. D. (1994). On the durability of pyrolytic carbon *in vivo*. *Medi. Prog. Technol.*, **20**, 201–208.
- Haubold, A. D., & Ely, J. L. (1995). *Carbons used in mechanical heart valves*. *Transactions Society for Biomaterials*. San Francisco: 21st Annual Meeting. 275.
- Haubold, A. D., Shim, H. S., & Bokros, J. C. (1981). Carbon in Medical Devices. In D. P. Williams (Ed.), *Biocompatibility of Clinical Implant Materials* (pp. 3–42). Boca Raton, Florida: CRC Press.
- Kaae, J. L., & Wall, D. R. (1996). Microstructural characterization of pyrolytic carbon for heart valves. *Cells Mater.*, **4**, 281–290.
- Kafesjian, R., Howanec, M., Ward, G. D., Diep, L., Wagstaff, L., et al. (1994). Cavitation damage of pyrolytic carbon in mechanical heart valves. *J. Heart Valve Dis.*, **3**(Suppl. I), S2–S7.
- Kelpetko, V., Moritz, A., Mlczech, J., Schurawitzki, H., Domanig, E., et al. (1989). Leaflet fracture in Edwards-Duromedics bileaflet valves. *J. Thorac. Cardiovasc. Surg.*, **97**, 90–94.
- King, R. N., Andrade, J. D., Haubold, A. D., & Shim, H. S. (1981). Surface Analysis of Silicon: Alloyed and Unalloyed LTI Pyrolytic Carbon. In D. W. Dwight, T. J. Fabish, & H. R. Thomas (Eds.), *Photon, Electron and Ion Probes of Polymer Structure and Properties*, *ACS Symposium Series* **162** (pp. 383–404). Washington, DC: American Chemical Society.
- LaGrange, L. D., Gott, V. L., Bokros, J. C., & Ramos, M. D. (1969). Compatibility of Carbon and Blood. In R. J. Hegyeli (Ed.), *Artificial Heart Program Conference Proceedings* (pp. 47–58). Washington, DC: US Government Printing Office.
- Lee, R. G., & Kim, S. W. (1974). Adsorption of proteins onto hydrophobic polymer surfaces: Adsorption isotherms and kinetics. *J. Biomed. Mater. Res.*, **8**, 251.
- Ma, L., & Sines, G. (1996). Fatigue of isotropic pyrolytic carbon used in mechanical heart valves. *J. Heart Valve Dis.*, **5**(Suppl. I), S59–S64.
- Ma, L., & Sines, G. (1999). Unalloyed pyrolytic carbon for implanted heart valves. *J. Heart Valve Dis.*, **8**(5), 578–585.
- Ma, L., & Sines, G. (2000). Fatigue behavior of pyrolytic carbon. *J. Biomed. Mater. Res.*, **51**, 61–68.
- More, R. B., & Haubold, A. D. (1996). Surface chemistry and surface roughness of clinical pyrocarbons. *Cells Mater.*, **6**, 273–279.
- More, R. B., & Silver, M. D. (1990). Pyrolytic carbon prosthetic heart valve occluder wear: *in vivo* vs. *in vitro* results for the Björk–Shiley prosthesis. *J. Appl. Biomater.*, **1**, 267–278.
- More, R. B., Kepner, J. L., & Strzepa, P. (1993). Hertzian Fracture in Pyrolite Carbon. In P. Ducheyne, & D. Christiansen (Eds.), *Bioceramics* Vol. 6, (pp. 225–228). Oxford, UK: Butterworth-Heinemann.
- Nyilas, E., & Chiu, T. H. (1978). Artificial surface/sorbed protein structure/hemocompatibility correlations. *Artif. Organs*, **2**(Suppl.), 56–62.
- Okazaki, Y., Wika, K. E., Matsuyoshi, T., Fukamachi, K., Kunitomo, R., et al. (1997). Platelets were early postoperative depositions on the leaflet of a mechanical heart valve in sheep without postoperative anticoagulants or antiplatelet agents. *ASAIO J.*, **42**, M750–M754.
- Pauling, L. (1964). *College Chemistry* (3rd ed). San Francisco, CA: W. H. Freeman and Company.
- Reilly, D. T., & Burstein, A. H. (1974). The mechanical properties of bone. *J. Bone Joint Surg. Am.*, **56**, 1001.
- Reilly, D. T., Burstein, A. H., & Frankel, V. H. (1974). The elastic modulus for bone. *J. Biomech.*, **7**, 271.
- Richard, G., & Cao, H. (1996). Structural failure of pyrolytic carbon heart valves. *J. Heart Valve Dis.*, **5**(Suppl. I), S79–S85.
- Ritchie, R. O., Dauskardt, R. H., Yu, W., & Brendzel, A. M. (1990). Cyclic fatigue-crack propagation, stress corrosion and fracture toughness behavior in pyrolite carbon coated graphite for prosthetic heart valve applications. *J. Biomed. Mat. Res.*, **24**, 189–206.
- Sadeghi, H. (1987). Dysfonctions des protheses valvulaires cardiaques et leur traitement chirurgical. *Schwiz. Med. Wochenschr.*, **117**, 1665–1670.
- Salzman, E. W., Lindon, J., Baier, D., & Merrill, E. W. (1977). Surface-induced platelet adhesion, aggregation and release. *Ann. NY. Acad. Sci.*, **283**, 114.
- Sattler, K. (1995). Scanning tunneling microscopy of carbon nanotubes and nanocones. *Carbon*, **7**, 915–920.
- Sawyer, P. N., Lucas, L., Stanczewski, B., Ramasamy, N., Kamlott, G. W., et al. (1975). Evaluation techniques for potential cardiovascular prosthetic alloys experience with titanium aluminum 6–4 ELI tubes. *Proceedings of the San Diego Biomedical Symposium*, Vol. 14, 423–427.
- Schoen, F. J. (1983). Carbons in Heart Valve Prostheses: Foundations and Clinical Performance. In M. Zychner (Ed.), *Biocompatible Polymers, Metals and Composites* (pp. 240–261). Lancaster, PA: Technomic.
- Schoen, F. J., Titus, J. L., & Lawrie, G. M. (1982). Durability of pyrolytic carbon-containing heart valve prostheses. *J. Biomed. Mater. Res.*, **16**, 559–570.
- Smith, K. L., & Black, K. M. (1984). Characterization of the treated surfaces of silicon alloyed pyrolytic carbon and SiC. *J. Vac. Sci. Technol.*, **A2**, 744–747.
- Stanley, J., Klawitter, J., & More, R. (2008). Replacing Joints with Pyrolytic Carbon. In P. A. Revell (Ed.), *Joint Replacement Technology: New Developments* (pp. 631–656). Cambridge, UK: Woodhead Pub and CRC Press LLC.
- FDA (US Food and Drug Administration) (2001). *Summary of Safety and Effectiveness, On-X® Prosthetic Heart Valve*. FDA PMA P000037 May 30.
- FDA (US Food and Drug Administration) (2002). *Summary of Safety and Effectiveness, On-X® Prosthetic Heart Valve*. FDA P000037/S1, March 6, 2002, European Primary Trial, updated May 31, 2003.
- Thompson, N. G., Buchanan, R. A., & Lemons, J. E. (1979). *In vitro* corrosion of Ti-6Al-4V and Type 316L stainless steel when galvanically coupled with carbon. *J. Biomed. Mater. Res.*, **13**, 35–44.
- Wieting, D. W. (1996). The Björk–Shiley Delrin tilting disc heart valve: Historical perspective, design and need for scientific analyses after 25 years. *J. Heart Valve Dis.*, **5**(Suppl. I), S157–S168.
- Williams, D. F. (1998). General Concepts of Biocompatibility. In J. Black, & G. Hastings (Eds.), *Handbook of Biomaterial Properties* (pp. 481–489). London, UK: Chapman and Hall.
- Williams, M. A., & van Riet, S. (2006). The On-X® prosthetic heart valve: Mid-term results in a poorly anticoagulated population. *J. Heart Valve Dis.*, **15**, 80–86.